Romanian Reports in Physics **69**, 802 (2017)

BIO-RETEXTURING IN LIMESTONE USED IN THE BUILT HERITAGE OF MALTA

LINO BIANCO

University of Malta, Faculty for the Built Environment, Msida MSD 2080, Malta,
E-mail: lino.bianco@um.edu.mt

Received February 27, 2017

Abstract. The paper addresses bio-retexturing within the Lower Globigerina Limestone, the limestone used in the construction of the island's built cultural heritage which dates back to the Neolithic Period. Samples from the host sedimentary layer and burrow infills were analysed to establish the varying petrological, geochemical and mineralogical charcateristics. Petrological examination in thin section indicates that burrowing introduces unlithified sediment in the primary depositional fabric. XRF and XRD indicate that the mineralogy of the infill is qualitatively and quantitatively different from the host rock, often richer in goethite which accounts for its dark yellow ochre colour. Bio-retexturing introduces predominantly non-carbonate rich infill and modifies the original sediment; due to the intra-particle cement, it transforms its permeability and porosity.

Key words: limestone, bio-retexturing, bioturbation, Globigerina Limestone, durability, weathering, architecture, Malta.

1. INTRODUCTION

Limestones are the most common industrial mineral utilised in the erection of architectural monuments since the Neolithic Period. Variations exist with location of deposition, and techniques are available to determine the provenance of the limestone utilised in such architecture [1]. Principal limestone characteristics and pathologies associated with its weathering in heritage buildings are imperative for effective damage diagnostics [2–3].

Burrows are an important characteristic of limestone. They are trace fossils formed within soft unconsolidated sediments and demonstrate the patterns, shapes and well-defined ichnofabrics [4]. Their diameter may vary from less than 1 mm to several centimetres [5]. The compaction of a given burrow can be computed in terms of [6].

In both shallow and deep marine environments, biota introduces displacement within the sediment and thus influences its composition [7]. Bioturbation involves the remixing of sediments by organisms, thus resulting in the obliteration of the original orientation of the sedimentary structures. It impacts on the porosity and permeability of the sediments [8]. Bioturbated and non-

bioturbated areas do have an impact on the weathering of the fabric. Limestone with bioturbation may exhibit greater weathering due to different porosity and related water capillary uptake.

Sediment bio-retexturing is the process by which biota burrowing in the substrate modifies and/or transforms the original sedimentary texture through the introduction of unlithified material of variable permeability and porosity from the host sediment of the lithostratigraphic layers [9]. It has a significant role within the lithostratigraphic layers [10]. "Bio-retexturing destroys [the] primary depositional fabrics and masks inorganic process-related structures" [9].

This paper studies the petrological, geochemical and mineralogical characteristics of samples extracted from Tal-Warda quarry on the outskirts of the geocultural village of Qrendi (UTM ED50 coordinates: 451481E, 3966547N), Malta, an open-pit industrial mineral extracting site sunk in the Lower Globigerina Limestone Member (LGLM) [11]. Burrowing and weathering activity is present (Fig. 1). The aim is not to quantify bioturbation but to investigate the qualitative and quantitative variations of the retextured infill to burrows from the respective lithostratigraphic layers.

The quarry is adjacent to the Chapel of St. Catherine (UTM ED 50 coordinates: 451486, 3966402N) (Fig. 2a,b) constructed in this limestone. This chapel (Fig. 2c,d), erected in 1626 and with its exterior restored in 2001, is a typical case study which illustrates burrowing in historic (Fig. 2e,g,h) and restored fabric (Fig. 2f). This chapel is listed in the *National Inventory of the Cultural Property of the Maltese Islands* for its 'very high' cultural heritage value due to its architectural, artistic and historical importance [12]. The Neolithic temples of Ħaġar Qim and Mnajdra, UNESCO World Heritage Sites dating to circa 3600 BC [13], are two of the many cultural heritage sites within the limits of this village.

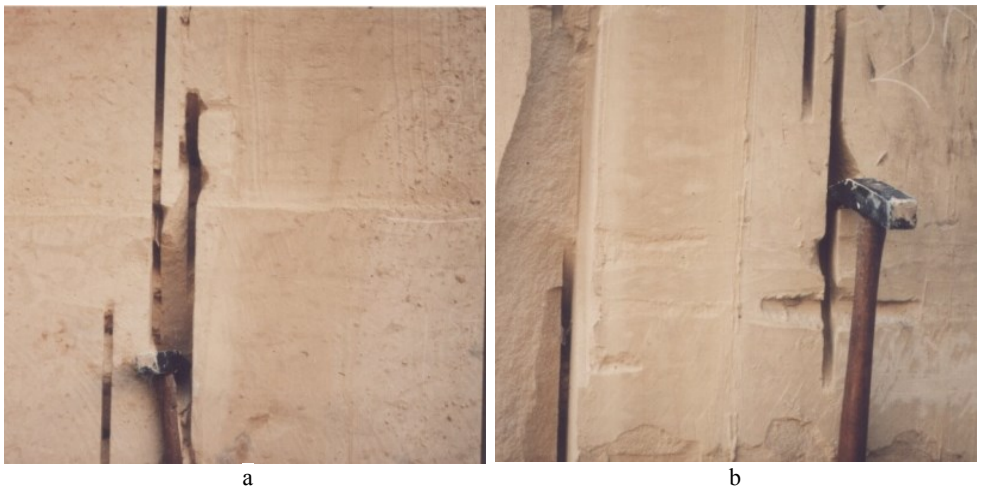

a b

Fig. 1

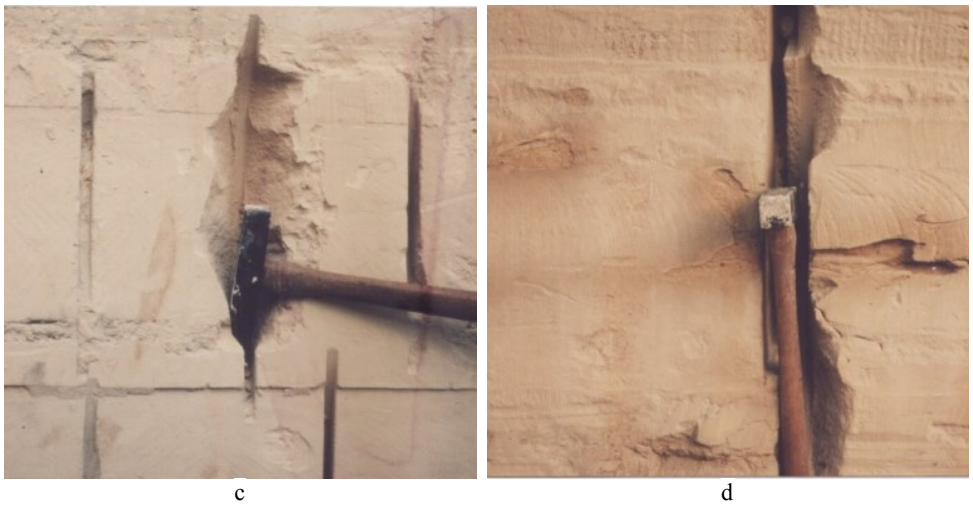

c d

Fig. 1 (continued) – Lower Globigerina Limestone (a) with burrowing (b) iron stained burrow infill (c) and weathering of burrow infill (d). For scale purposes, the head of the geological hammer is 160 mm long.

2. MATERIALS AND METHODS

The Lower Globigerina Limestone is the main building dimension stone in the Maltese islands. Even over a few kilometres the quality of this limestone varies, an important consideration when selecting limestone for stone replacement in any restoration work [14].

The geology of the Maltese archipelago consists of five main Oligo-Miocene formations of marine sedimentary origin [15]. These are, starting from the oldest, Lower Coralline Limestone Formation, Globigerina Limestone Formation, Blue Clay Formation, Greensand Formation and the Upper Coralline Limestone Formation. The Globigerina Limestone Formation, which outcrops over circa 70% of the superficial area of the islands, consists of pale cream to yellow planktonic globigerinid foraminifera. Lithostratigraphically it is divided into three members: Lower, Middle and Upper. The interruption in the process of sedimentation between these members is marked by two distinct, principal conglomerate beds. The LGLM is Aquitanian [16–17]; its thickness varies between 5 and 40 m [11] and this member has occasional blue patches [18]. Its bio-chronostratigraphy is characterized by calcareous plankton [19]. The alveolar weathering which characterises this member is due to selective intra-burrow cementation and preferential erosion of the surrounding poorly cemented sediment [15]. The resulting profile of preferential weathering in areas with burrows has been

traditionally referred to by quarrymen as ‘finger marks’ (Salvatore Bondin, personal communication), in Maltese ‘marki tas-swaba’. The top of Tal-Warda quarry is close to the upper limit of the LGLM and thus close to the lower side of the phosphorite conglomerate horizon. The top of this horizon marks the lower limit of the Middle Globigerina Limestone Member.

A comprehensive study of the LGLM was undertaken at the University of Leicester [20]. This limestone is either of the first or of the second, and inferior, quality type. The dominant mineralogy common to both is calcite with minor inclusions, which are more pronounced in the latter quality type, of quartz, K-feldspar, muscovite, kaolinite, illite, smectite and glauconite. This paper is based on the following 6 samples, analysed in [20] but not yet published: 3 host rock (R1 to R3) and their respective burrow infills (Rbf1 to Rbf3). R1 is second quality whilst R2 and R3 are first quality. The quarry face and hand specimen rock descriptions are given in Table 1. The petrological composition of the samples was established through textural, chemical and mineralogical analyses.

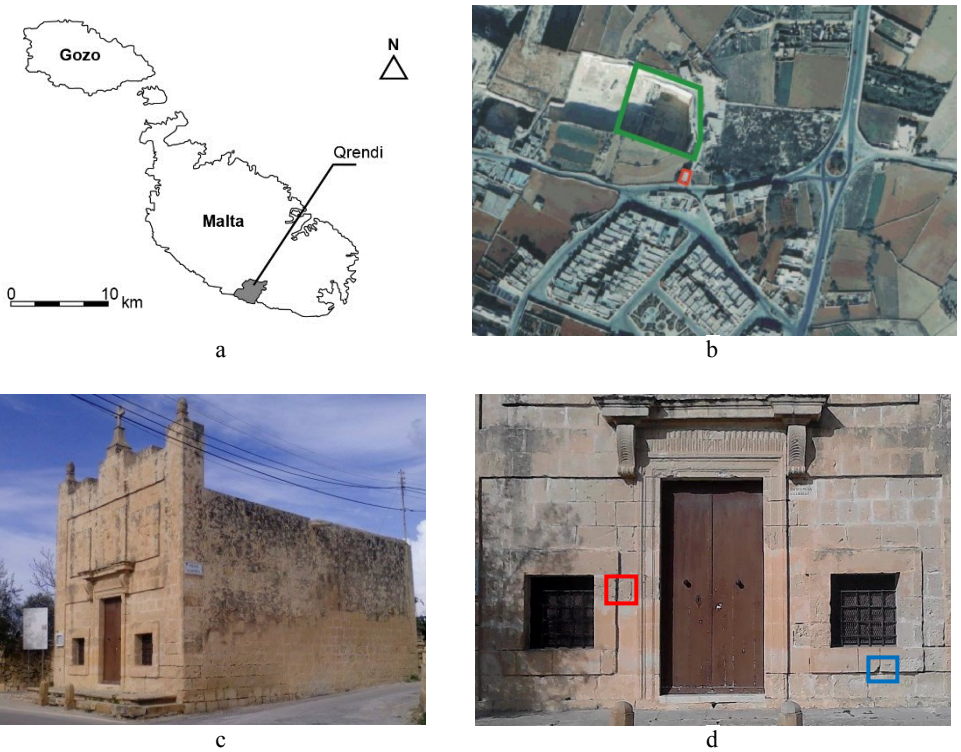

Fig. 2

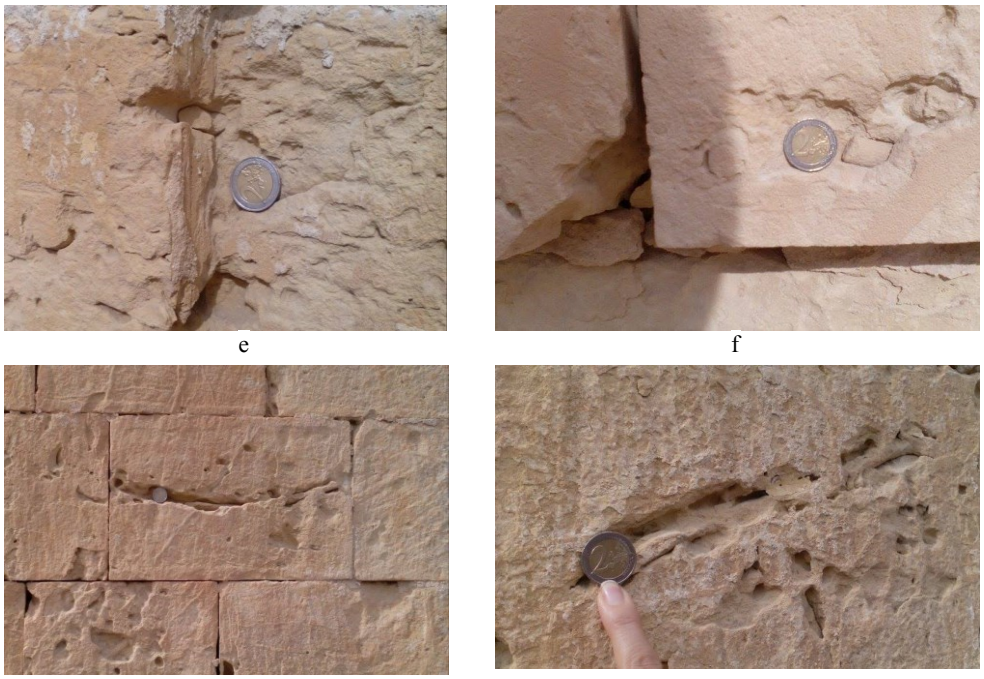

e f

g h

Fig. 2 (continued) – Location of the Neolithic village of Qrendi (a); orthophoto of the site plan [21]: Chapel of St. Catherine and the Tal-Warda Quarry are outlined in red and blue respectively (b); the Chapel of St. Catherine (c); detail of south-facing elevation of the chapel (d); burrowing in the original historic fabric indicated in red in Fig. 2d (e); burrowing in the restored fabric indicated in blue in Fig. 2d (f); burrowing in the original historic fabric along the east facing elevation (g, h). A 2€ coin was placed against the photographed fabric to illustrate the scale of the burrows.

A petrographical microscope and a Hitachi S-520 scanning electron microscope equipped with an energy-dispersive analyzer for high-resolution imaging were used. The objective of thin section analysis was to investigate the texture, porosity and permeability, important properties of a given limestone which have a bearing on its durability and weathering characteristics. These are essential aspects which need to be addressed in scientific restoration of historical built fabric.

Scanning electron microscopy (SEM) was also used to study the texture, the cementing fabric, the microphotograph pores [22] and the non-carbonate fraction remaining on the filter paper after the determination of the acid insoluble residue (IR). To avoid contamination, fragments were freshly cut and handled by disposable gloves and tongs. Furthermore, to guarantee electrical contact between the sample and the specimen pin mount, a gold coating was applied to secure a clear image.

Table 1

Visual descriptions

Code	Position from quarry top (m)*	Bed thickness (m)*	Description	
			Quarry face	Hand specimen
R1	13.1	3.0	Darker burrow infill decreasing towards the top	White in colour with some shell fragments; Burrows: brown and dark green/grey in colour with occasional 'iron stained' infill
R2	20.7	3.2	Dark burrow infill starts at boundary with the lower bed; it increases up the bed; poor first quality is deteriorating upwards	Pale yellow coloured; Host rock is first quality but burrows reduce quality
R3	28.1	6.0	Host rock is first quality but with darker soft yellow infill to burrows; progression increases up in the bed	Pale yellow coloured with shell fragments; Burrows: cream yellow infill; seems more compact than the host rock

* Approximate depth in metres.

Chemical analysis was determined through loss-on-ignition (LOI), the traditional analytical chemical method used to establish the organic and carbonate content of a given sediment [23], and X-ray fluorescence analysis (XRF). An ARL 8420+ X-ray fluorescence spectrometer was used to determine the bulk chemistry [24]. Pressed powder pellets were analysed for SiO_2, TiO_2, Al_2O_3, Fe_2O_3, MnO, MgO, CaO, Na_2O_3, K_2O, and P_2O_5.

The non-carbonate fraction present was quantitatively determined through IR. X-ray diffraction (XRD) making use of a Philips PW1729 X-ray generator was used to determine the mineralogical composition of the residue. XRD was also used to qualitatively establish the bulk mineralogy of the whole rock samples and the mineralogy of the clay fractions. The respective relative intensities are indicative of the semi-quantitative data of each mineral. An oriented mount technique was used to prepare the clay minerals in order to enhance the d001 peaks [25].

3. RESULTS AND DISCUSSION

The host rock and burrow infill samples consist of fine grained, well-sorted, porous intrabiosparitic wackestone. SEM images show the pore structure, and fine grained cement with occasional well-formed minerals (Fig. 3).

Burrows, when present, have compact, low porosity wackestone infill. In R1, burrows cut across the section; the fabric of the infill is similar to that of the host. Compact, low porosity 700 μm diameter areas, likely sections through the infill to

burrows, are present. The maximum size of fossil fragments is 0.68 mm. Quartz, maximum size of 75 µm, occurs in clusters and maximum 150 µm diameter glauconite grains are also present. 350 µm maximum diameter clusters of iron oxide-like minerals, dark red-brown in colour and exhibiting signs of breakdown, often occur in concave-up position shells. Glauconite grains in the oxide stained areas are breaking down. Burrows in R2, diameter varying from 0.75 to 2 mm, do not cut across the fabric. Infill is low in unbroken allochem content, less compact and low in porosity. Iron oxide minerals in proximity to areas of high permeability are breaking down. Quartz size ranges from 20 to 120 µm. Glauconite grains are not breaking down.

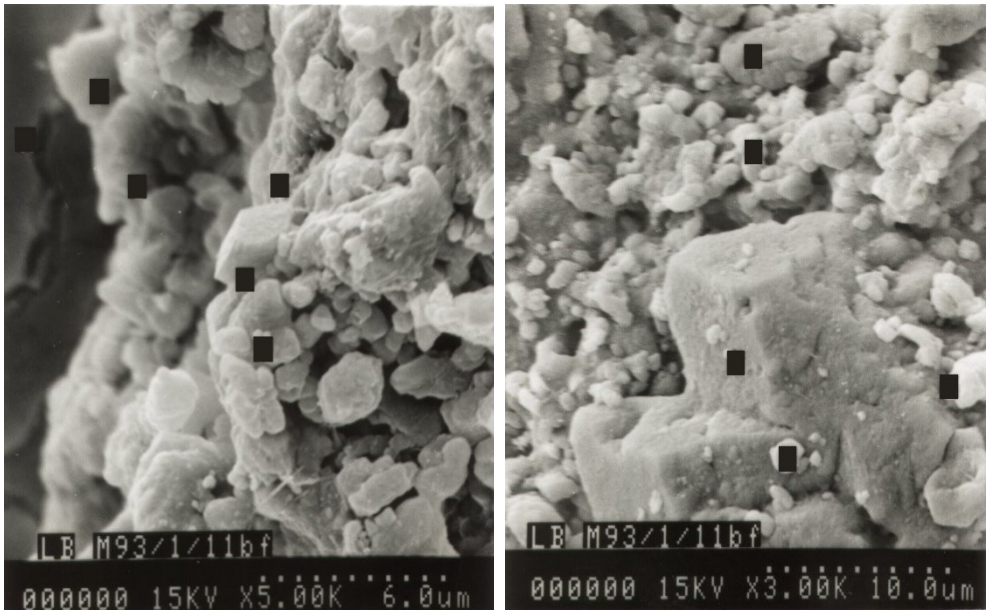

a b

Fig. 3 – Scanning electron images showing the pore structure of sample Rbf2 (a); a well defined feldspar is present (b). ■ indicates points analysed.

Undamaged, unfilled globigerina comprises 30% of R3. Maximum diameter of undamaged allochems is 675 µm. Other minerals present include glauconite, quartz and some oxides. Well defined glauconite grains, maximum 20 µm diameter, are present in intra particle pores. They also occur in clusters over an area of 250 × 125 µm. Quartz grains, maximum 90 µm, are scattered throughout the fabric. 7.5 µm diameter red-brown iron oxide mineral grains are uniformly distributed throughout the fabric. Some are starting to break down and staining the surroundings. Some of the globigerina chambers are filled with this mineral. Green-grey stains may be due to weathering of glauconite. High permeability areas

are severely stained; breakdown of glauconite is more advanced in these areas. Inter particle pores are maximum 400 μm in diameter. Elongated quartz, maximum 100 μm, occurs occasionally in groups. 5 to 10 μm iron oxide mineral grains occur in clusters; sometimes they are contained in allochem chambers. The maximum inter particle oxide cluster is 85 μm. Oxide filled allochem chambers have sparry calcite on the inside of the chamber.

The bf sample viewed in thin section is Rbf3. Allochems are cemented by fine-grained sparry calcite. Secondary 1.5 mm diameter burrows cut across the primary burrow fabric. Infill to a secondary burrow is more permeable. A number of iron oxide mineral(s) is/are present at the boundaries of the secondary burrow. Size is difficult to establish due to intense staining around the mineral core which blurs the perimeter of the grain.

Nearly a third of the host rock is made up of undamaged, unfilled allochems (maximum 150 μm diameter). The remaining area includes laminar shell fragments (maximum size 1 mm), glauconite grains (10% of fabric and 200 μm maximum diameter), quartz and iron oxide/s. Well-defined glauconite grains, occurring in groups, fill intra particle voids. Shell fragments in concave-up position support glauconite grains. Monocrystalline quartz grains are elongated and angular. Their size varies from 20 to 120 μm. Irregular distributed breaking down 30 μm iron oxide mineral is also present; staining is due to red-brown iron oxide and glauconite break down. The secondary burrow infill is less stained than the host burrow infill.

The geochemical composition of the R samples varies from the Rbf samples (Table 2). The LOI content of all samples is less than the theoretical value for pure $CaCO_3$. The samples with burrow infill have lower LOI content than that of the host rock. The noted mean variation is circa 4%. Bioturbation had introduced different amounts of oxides in the infill which are not present in the respective host lithostratigraphic layer.

Table 2

XRF analysis of samples

	R1	R2	R3	Rbf1	Rbf2	Rbf3
SiO_2	06.506	04.272	05.094	03.103	08.573	09.310
TiO_2	00.117	00.070	00.084	00.042	00.122	00.134
Al_2O_3	00.838	00.434	00.513	00.876	01.032	01.126
Fe_2O_3	00.822	00.317	00.633	00.410	01.392	01.497
MnO	00.035	00.036	00.036	LOD*	00.036	00.038
MgO	01.173	00.719	01.172	00.730	01.010	01.359
CaO	49.577	50.222	48.789	51.592	45.424	46.253
Na_2O_3	00.055	00.071	00.141	00.423	00.495	00.298
K_2O	00.369	00.185	00.251	00.216	00.540	00.548
P_2O_5	00.707	00.186	01.080	00.172	04.001	03.257

* LOD: below limits of detection.

Burrow infill in the first quality bed has lower CaO and higher non-carbonate oxides than the host rock, that is, bioturbation has introduced a new matrix of non-carbonate SiO_2 and P_2O_5 rich sediment in the burrows. A marked increase in Fe_2O_3, Al_2O_3 and K_2O is also noted. Whilst negligible variation is present in the MnO content, Na_2O_3 is significantly higher, nearly 600% more than in the host rock. With respect to the second quality limestone, this oxide in the corresponding burrow infill Rbf1 is circa 700%. This sample registered a higher CaO content and a decrease in all non-carbonate fraction with the exception of Al_2O_3 which registered a negligible increase. XRD recorded the presence of calcite and quartz in all samples (Table 3 and Fig. 4). The mineralogy of the insoluble residue is mainly quartz and K-feldspar. Muscovite, rutile and albite were detected. Kaolinite, illite and smectite were also recorded. Goethite was noted in both first and second quality burrow infills. It is a weathering product of iron bearing minerals. The mineralogy of the clay fraction in the R2 and Rbf2 samples is kaolinite, illite, smectite, quartz and K-feldspar.

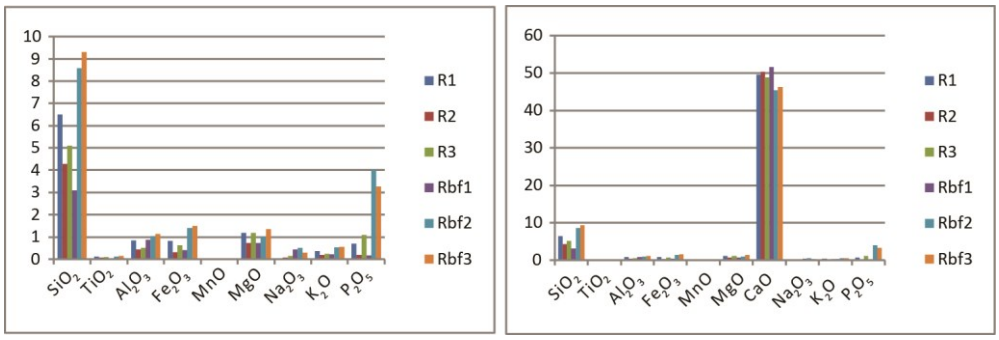

a b

Fig. 4 – Percentage distribution of the geochemical composition of the non-carbonate fraction (a) together with CaO (b).

Table 3

Minerals identified through XRD

		R1	R2	R3	Rbf1	Rbf2	Rbf3
Whole rock	calcite	x	x	x	x	x	x
	quartz	x	x	x	x	x	x
Insoluble residue	quartz	x	x	x	x	x	
	K-feldspar	x	x	x	x	x	x
	muscovite	x		x		x	
	kaolinite	x			x		
	illite						x
	smectite						x
	goethite				x	x	
	rutile			x			

Table 3

(continued)

Insoluble residue		R1	R2	R3	Rbf1	Rbf2	Rbf3
	albite		x				
	zeolite				x		
Clay fraction	kaolinite		x			x	
	illite		x			x	
	smectite		x			x	
	quartz		x			x	
	K-feldspar		x			x	

4. CONCLUSION

Petrological examination indicates that burrowing activity introduces unlithified sediment of variable permeability in the host rock. Bioturbation introduces weaknesses and unstable material into the host lithostratigraphic fabric.

XRF and XRD analyses of the LGLM indicate that the variations in the geochemistry and the mineralogy of the burrow infill from the lithostratigraphic bed are both qualitative and quantitative. Burrows are filled by mineralogically different sediments from the host lithostratigraphical layer, the primary depositional fabric. They may be rich in goethite which accounts for the dark yellow ochre like colour of the infill and the distinct brown ferruginous staining of the fabric.

Findings are in line with [9]. Bio-retexturing introduces unlithified sediment, predominantly non-carbonate rich infill. It modifies the original sediment and, due to the intra-particle cement, transforms its permeability and porosity. This has a bearing on the capillary water intake which impinges on the weathering of the fabric. The texture of bioturbated and non-bioturbated areas varies significantly.

The composition and the cement of the initially unlithified sediment introduced through bio-retexturing are of significant importance in the preservation and consolidation of deteriorated building stone.

Acknowledgements. The author wishes to thank Dr. Hugh Martyn Pedley and the late Professor Anselm Dunham for their advice while this study was being undertaken. Thanks are also due to Alessandra Bianco for her support during the course of preparing this publication. This research was funded by the Oil Exploration Division, Office of the Prime Minister, Malta.

REFERENCES

1. L. Bianco, *Techniques to determine the provenance of limestone used in Neolithic architecture of Malta*, Romanian Journal of Physics **62**, 901 (2017).
2. A.-A. Balog, N.Cobirzan, E. Mosonyi, *Analysis of limestones from heritage buildings as damage diagnostics*, Romanian Reports in Physics **68**, 353–361 (2016).

3. E. Torrero, D. Sanz, M.N. Arroyo, V. Navarro, *The Cathedral of Santa Maria (Cuenca, Spain): Principal stone characterization and conservation status*, International Journal of Conservation Science **6**, *4*, 625–632 (2015).
4. R. G. Bromley, *Trace Fossils. Biology, Taphonomy and Applications*, Chapman & Hall, London, 1996.
5. S.S. Das, C.N. Rao, *Micro-burrows from the Charmuria Formation, Madhya Pradesh, India*, Palaios **7**, 548–552 (1992).
6. W. Ricken, *The carbonate compaction law: a new tool*, Sedimentology **34**, *4*, 571–584 (1987).
7. E. Flugel, *Microfacies of Carbonate Rocks: Analysis, interpretation and application*, Springer, 2004, pp. 185–190.
8. M.K. Gingras, G. Baniak, J. Gordon, J. Hovikoski, K.O. Konhauser, A. La Croix, R. Lemiski, C. Mendoza, S.G. Pemberton, C. Polo, J. P. Zonneveld, *Porosity and permeability in bioturbated sediments*, in D. Knaust, R.G. Bromley (Eds.), *Trace Fossils as Indicators of Sedimentary Environments. Developments in Sedimentology*, **64**, Elsevier, 2012, pp. 837–868.
9. H. M. Pedley, *Bio-retexturing: early diagenetic fabric modifications in outer-ramp settings – a case study from the Oligo-Miocene of the Central Mediterranean*, Sedimentary Geology **79**, 173–188 (1992).
10. M. J. O'Leary, C. T. Perry, S. J. Beavington-Penney, J. R. Turner, *The significant role of sediment bio-retexturing within a contemporary carbonate platform system: Implications for carbonate microfacies development*, Sedimentary Geology **219**, *1*, 169–179 (2009).
11. Oil Exploration Division, *Geological Map of the Maltese Islands*. Office of the Prime Minister, Malta, 1993.
12. Superintendence of Cultural Heritage, *National Inventory of the Cultural Property of the Maltese Islands*, Inventory No. 01252, http://www.culturalheritage.gov.mt/filebank/inventory/Chapels%20and%20Niches/01252.pdf. Accessed on 19.10.2016.
13. UNESCO, *World Heritage List: Megalithic Temples of Malta*. http://whc.unesco.org/en/list/132. Accessed on 30.03.2016.
14. L. Bianco, *Limestone replacement in restoration: The case of the church of Santa Maria (Birkirkara, Malta)*, International Journal of Conservation Science **8**, *2*, 167–176 (2017).
15. H.M. Pedley, M.R. House, B. Waugh, *The Geology of Malta and Gozo*, Proceedings of the Geologists' Association **87**, *3*, 325–341 (1976).
16. R. Felix, *Oligo-Miocene Stratigraphy of Malta and Gozo*, H. Veenman and B.V. Zonen, Wageningen, 1973.
17. L. Giannelli, G. Salvatorini, *I foraminiferi planctonici dei sedimenti Tertiari dell`archipelago Maltese*, Atti della Societa` Toscana di Scienze Naturali, Memorie, Serie A **79**, 49–74 (1972).
18. L. Bianco, *Mineralogy and geochemistry of blue patches occurring in the Globigerina Limestone Formation used in the architecture of the Maltese Islands*, Comptes rendus de l'Académie Bulgare des Sciences **70**, *4*, 537–544 (2017).
19. N. Baldassini, R. Mazzei, L.M. Foresi, F. Riforgiato, G. Salvatorini, *Calcareous plankton bio-chronostratigraphy of the Maltese Lower Globigerina Limestone member*, Acta Geologica Polonica **63**, *1*, 105–135 (2012).
20. L. Bianco, *Some Factors Controlling the Quality of Lower Globigerina Building Stone of Malta*, Unpublished M.Sc. Dissertation, University of Leicester, Leicester, 1993.
21. Planning Authority, *Orthophotos/Orthos 1998*, http://geoserver.pa.org.mt/publicgeoserver. Accessed on 21.11.2016.
22. S.J.B. Reed, *Electron Microscope Analysis and Scanning Electron Microscopy in Geology*, Cambridge University Press, 2005.

23. W.E. Dean, *Determination of carbonate and organic matter in calcareous sediments and sedimentary rocks by loss on ignition: comparison with other methods*, Journal of Sedimentary Petrology **44**, 242–248 (1974).
24. G. Fitton, *X-ray fluorescence spectrometry*, in R. Gill (Ed.), *Modern Analytical Geochemistry*, Longman, 1997, pp. 97–115.
25. J. I. Drever, *The Preparation of Oriented clay Mineral Specimens for X-ray Diffraction Analysis by a Filter-Membrane Peel Technique*, American Mineralogist **58**, 553–554 (1973).